J Ther Eng, Vol. 10, No. 5, pp. 1184−1197, September, 2024

Journal of Thermal Engineering
Web page info: https://jten.yildiz.edu.tr
DOI: 10.14744/thermal.0000860

Research Article

Optimizing the thermal performance of a double-pipe heat exchanger using twisted tapes with variable cuts and Fe_3O_4 nanofluid

K. P. V. Krishna VARMA[1], N. S. NAVEEN[2], P. S. KISHORE[3,*], Satish PUJARI[2], Krishna JOGI[4], V. Dhana RAJU[5]

[1]Department of Mechanical Engineering, Raghu Engineering College, Visakhapatnam, Andhrapradesh, 531162 India
[2]Department of Mechanical Engineering, Lendi Institute of Engineering and Technology (A), Vizianagaram, Andhra Pradesh, 535005, India
[3]Department of Mechanical Engineering, Andhra University College of Engineering (A), Andhra University, Visakhapatnam, 530003, India
[4]Department of Mechanical Engineering, Rise Krishna Sai Prakasam Group of Institutions, Ongole, Andhra Pradesh, 523272, India
[5]Department of Mechanical Engineering, Lakireddy Balireddy College of Engineering (A), Mylavaram, Andhra Pradesh, 521230, India

ARTICLE INFO

Article history
Received: 06 September 2023
Revised: 28 November 2023
Accepted: 04 December 2023

Keywords:
ANN; Cut Twisted Tapes; Friction Factor; Nanofluid; Nusselt Number; Reynolds Number; Taguchi

ABSTRACT

This research work aims to optimize double pipe heat exchanger performance using Taguchi, ANOVA, and ANN. Experimental trials involved varying ferric oxide nanoparticles, cut radius, and volume-based flow rate. Twisted tapes with ratios of 3, 5, and 7 were placed within the tube. Assessed heat transfer characteristics included h, Nu, ff, and thermal performance factor. Taguchi, ANOVA, and ANN optimization techniques were applied to the experimental data. A Taguchi optimization using an L9 orthogonal array focused on input attributes (Vol % of nanoparticles, flow rate, radius of cut), with output attributes being heat transfer co-efficient (h), Nusselt number (Nu), friction factor(ff) and thermal performance factor. Results revealed a notable flow rate effect on enhancing h, Nu, and ff, while the addition of nanoparticles significantly influenced thermal performance. Taguchi and ANOVA were conducted using MINI Tab and ANN was implemented through MATLAB. Test data demonstrated that nanoparticle dispersants in nanofluid significantly improved heat transfer properties, consistent with the noteworthy improvement indicated by optimization techniques. The convective heat transfer coefficient parameter showed improvement with a coolant flow rate of 50.29% and a volume of nanoparticles at 27.32%. The enhancement of Nusselt number (Nu) was influenced by a coolant flow rate of 50.34% and a volume percent of nanoparticles at 34.25%. The thermal performance factor was significantly influenced by the volume percent of nanoparticles (79.75%) and the radius of cut (3.83%).The experimental data aligned well with findings from Taguchi and ANN.

Cite this article as: Varma KPVK, Naveen NS, Kishore PS, Pujari S, Jogi K, Raju VD. Optimizing the thermal performance of a double-pipe heat exchanger using twisted tapes with variable cuts and Fe_3O_4 nanofluid. J Ther Eng 2024;10(5):1184−1197.

***Corresponding author.**
*E-mail address: psrinivaskishore@gmail.com, prof.pskishore@andhrauniversity.edu.in

This paper was recommended for publication in revised form by Editor-in-Chief Ahmet Selim Dalkılıç

Published by Yıldız Technical University Press, İstanbul, Turkey

INTRODUCTION

Food processing, oil and gas, chemical industries, power plants, and other industries widely use double-pipe heat exchangers. Escalation in rate of heat transfer in heat exchangers leads to compactness, energy savings, and cost reductions. There are various approaches to augmenting the amount of heat exchange in heat exchange devices. These techniques are broadly classified into three categories. The first category includes active approaches that require an external source of energy. Active approaches include mechanical aids, surface aids, electrostatic fields, jet impingement and sprays. The passive techniques fall under the second group, as they do not rely on external power. Twisted tapes, dimples, ribs, wire coils, and other techniques are examples of these techniques. The compound approach, which combines two passive or two active techniques, or a combination of active and passive techniques, is the third category of intensification methods reported by Bergles [1]. Traditional heat transfer fluids contain a lower Thermal conductivity (k), to improve the fluid's thermal conductivity; nanoparticles are dispersed in the carrier fluid. The thermal conductivity of carrier fluids is increased by suspending lower-volume concentrations of solid nanoparticles in the carrier fluid. A fluid with nanometer-sized particles containing colloidal suspensions made of carrier fluid and nanoparticles is referred to as a nanofluid. Metals, oxides, and carbon nanotubes are the most common nanoparticles using water, ethylene glycol, or oil as the carrier fluid. In comparison to the carrier fluid, nanofluids have a higher thermal conductivity revealed by Buongiorno [2], Godson et al. [3] and Bozorg Bigedli et al. [4]. Localized heat transfer, the surface charge possessed by the particles, increased conductive ability, and the Brownian motion of the nanoparticles were some of the elements that contributed to the enhanced capabilities of nanofluids according to the Kakac and Pramuanjaroenkij [5]. Nanofluids are used in a variety of industries, including medicine, electronics, thermal processing and solar energy applications, due to their superior heat transfer qualities. These fluids can also be employed in cooling applications as heat transfer fluids. Nanofluids are also interesting prospects for mass transportation, optical devices, increased critical heat flux and light-water reactors inferred by Sarafraz et al. [6, 7] and Shima et al. [8].

Chopkar et al. [9] used 4.7 percent ferric oxide nanofluids to achieve a 30% increase in thermal conductivity. Parekh and Lee [10] stated that when CuO nanoparticles were added to ethylene glycol, thermal conductivity was found to increase by 20%. Under laminar flow, an attempt by Syam Sundar et al. [11] was made to investigate the influence of ferric oxide nanofluids generated with vacuum pump oil as the basis fluid. In comparison to the carrier fluid, the nanofluids resulted in a 17.83 percent increase in heat transmission. Han et al. [12] studied how an Al_2O_3 nanofluid would affect a heat exchanger with two pipes. According to the study findings, heat transmission improves as temperature and nanoparticle concentration rise. The Nusselt number is shown to have increased by 24.5 percent. Guan et al. [13] explored the efficacy of magnetic nanofluids in enhanced oil recovery technology, investigating the impact of nanoparticle synthesis through the sol-gel method within the 10–90 nm range at different temperatures. Findings revealed a 10% higher oil recovery with nanoparticles prepared at 300°C compared to those prepared at 600°C in the study. Elsaidy et al. [14] investigated the thermal conductivity (k) of Fe_2O_3 nanofluid clusters. This thermal approach to make nanoparticles with a cluster size of 46–240 nm and concentrations varying from up to 1.5 percent. With 240 nm nanoparticles, a maximum increase of 4.4 percent in thermal conductivity was achieved.

A plain pipe positioned with twisted tapes in combination with single-phase fluid improves heat transfer and pressure drop, according to several types of research [15-19]. A mathematical study by Varma et al. [20], on the heat exchanger of a twin-type with perforated and geometry-modified perforated inserts, found a noteworthy improvement in heat transfer with the geometry-modified tube inserts with perforations compared to the plain pipe. Kelidari et al. [21] investigated how a curved pipe performed when using Fe_3O_4 nanofluid. The parameters of heat transfer found in a pipe containing nanofluid had improved. Syam Sundar et al. [22] conducted trials to evaluate the impact of full-length twisted tapes and ferric oxide nanofluid in a tube with various particle volume concentrations and twist ratios. Results revealed that, compared to the simple pipe, there is a 58 percent rise in the amount of heat transfer. Al_2O_3 nanofluid was employed by Aghayari et al. [23] to evaluate the heat exchanger efficacy of twin-pipe following the experiments; it was revealed that nanofluid heat transmission is 12 percent larger than base fluid. Aghayari et al. [24] assessed the effect of a twin-type heat exchanger employing Fe_2O_3 nanofluid in an experimental study. In light of the findings, the ability of the base fluid to transport heat is improved when nanoparticles were added. Wijayanta et al. [25] established that the pipe equipped with a cut-twisting square-shaped tube insert with twist ratios of 2.7, 4.5 and 6.5 resulted in a 45.5-80.5 percent and 2.0-3.3 times intensification in parameters like ff and Nu, respectively. They reported thermal performance factor is 1.23, which is the greatest, in comparison to tubes without twisted tape inserts. Al-Obaidi [26] did a numerical analysis on circular pipes through CFD.After obtaining the results from the CFD, the data were optimised with Taguchi. The data obtained from Taguchi and CFD is in good agreement. Kumar and Sahoo [27] conducted an experimental study on a heat exchange device of wavy-fin and tube with air. The outcomes revealed that the test results and the optimized data were in good alignment when the data obtained from the trial was compared to Taguchi data. Kavitha et al. [28] studied the heat transfer behaviour of a double pipe heat exchanger experimentally by passing copper based nanofluid through the pipe. Results reveal that the Vol% of Cu nanoparticles increases there is a significant improvement

in the thermal performance of a heat exchanger increases. Praveenkumara et al. [29] studied the behaviour of a double pipe heat exchanger by considering the twisted tape and threaded pipe. Experiments were conducted on the heat exchanger by passing the water through the pipe. Results reveals that there is a twisted tape inserted pipe and threaded pipe shown a greater enhancement of Nusselt number while compared to the smooth pipe. Colaco et al. [30] studied the improvement of thermal performance of a heat pipe experimentally and optimized with NSGA-I and NSGA-II. Results shown that there is a significant augment in heat transfer rate with baffles in a heat exchanger while compared to the heat exchanger without baffles.

Cut and twisted tapes have been used in a variety of works. Several researchers have looked into different cut forms. Heat transfer in heat exchangers has become more intense; it is caused by changes in the geometry of twisted tapes and each variation in the twisted tape geometry is unique and provides an enhancement differently. Many studies have looked into how twisted tapes can improve the transmission of heat in a plain pipe [15-20]. Numerous data on nanofluids, whole-length twisted tapes with single-phase fluid and full-length sliced twisted tapes with single-phase fluid can be found in the literature. Optimization through Taguchi and ANN on DPHE placed with variable-cut inserts using ferric oxide nanofluid was found to be very rare and experimental study of a DPHE by using ferric oxide nanofluid at 0.01,0.03 and 0.05 Vol% was rare hence the aforementioned reasons to explore the current study. The goal of this work is to look into the h, ff, Nu and thermal performance factor of a Fe_3O_4-based nanofluid under turbulent flow regimes using a plain pipe with cut twisted tapes of shorter length in a twin pipe heat exchanger. In addition to that, optimization through Taguchi and ANN was done on the experimental data. To the best of the knowledge, only a few researchers have considered the combination of two methods, active and passive, to augment the rate of heat transfer in heat exchangers. This work intends to fill this gap by combining the nanofluids & cutting in twisted tape to augment the transfer of heat and optimized the trial data by considering the how input attributes like flow rate, Volume percentage of nanoparticles and radius of cut influences in the performance variables like h, Nu, ff and Thermal performance factor in a heat exchanger.

In the current work, Initially Ferric oxide nanofluid was prepared by two-step method described in section 2.1., the detailed description of experimental setup i.e. double pipe heat exchanger, dimensions of twisted tapes with various h/d ratio was represented in section 3.Formulae used in evaluating the heat transfer parameters of a heat pipe were represented; validation of heat pipe and uncertainty analysis was completely represented in sections 3.1-3.4. Where section 4 completely provides the results and discussions i.e. data obtained from different optimization techniques like Taguchi and ANN.

MATERIALS AND METHODS

Preparation of Fe3O4 Nanofluids

Ferric oxide (Fe_3O_4) nanoparticles of size 50-100 nm were procured from Hychem Laboratories, Hyderabad. A pictorial perspective on the procured Fe_3O_4nanoparticles is depicted in Figure 1. For the current work, the necessary quantity of the nanoparticles of various Vol fractions i.e. in between 0.01-0.05 % be estimated by using Eq. [1] suggested by Syam Sundar et al. [22]

$$\emptyset_{pv} = \frac{\frac{W_{Fe_3O_4}}{\rho_{Fe_3O_4}}}{\frac{W_{Fe_3O_4}}{\rho_{Fe_3O_4}} + \frac{W_{water}}{\rho_{water}}} \quad (1)$$

XRD investigation was done to evaluate the average size of nanoparticles with the help of Scherer Eqn. (2) and it is found to be 26.97 nm.

$$D = \frac{K\lambda}{\beta Cos\theta} \quad (2)$$

Fe_3O_4-based nanofluid was prepared by considering the base fluid as water. The difference in density between base fluid and nanoparticles tends to be high because when nanoparticles are suspended in the base fluid, they tend to agglomerate. To avoid this agglomeration, traditionally, surfactant was used to synthesize highly stable nanofluid.

The required quantity of Fe_3O_4-based nanofluid was prepared. Initially, the necessary quantities of nanoparticles were added step by step to prepare the different volume fractions of nanofluid. The base fluid was treated with sodium lauryl sulfate as a surfactant, and the mixture was then ultrasonically processed for about three hours using an ultrasonicator to obtain a highly stable nanofluid, as illustrated in Figure 1(a). Figures 1(b) and 1(c) illustrate the SEM and EDAX images of Fe_3O_4 nanoparticles.

Description of Cut Twisted Tapes

Aluminum is used to make twisted tapes, which have dimensions of 1.5 x 0.017 m. Table 1 lists the information about the twisted tapes. Where 'h', 'd' and 'r' denote the length, width, and radius of the twisted tape. Two twisted tapes, each 1 meter in length, were positioned into the tubes of the heat exchanger.

A 0.002-inch gap is left between the tape's edge and the tube's interior wall to make it easier to put the tape inside. The mechanical twister's lathe receives one end of the aluminium strip, which is then fastened there to be twisted. Twist ratios of h/d = 3, 5 and 7 have been assessed. The mass flow rate of the nanofluid circulated in the tube with twisted tapes can be calculated using the internal pipe diameter. The inner diameter of the pipe is determined by the hydraulic pipe diameter.A photographic view of varying cross-section cut (VCSC) and varying cut (VC) twisted

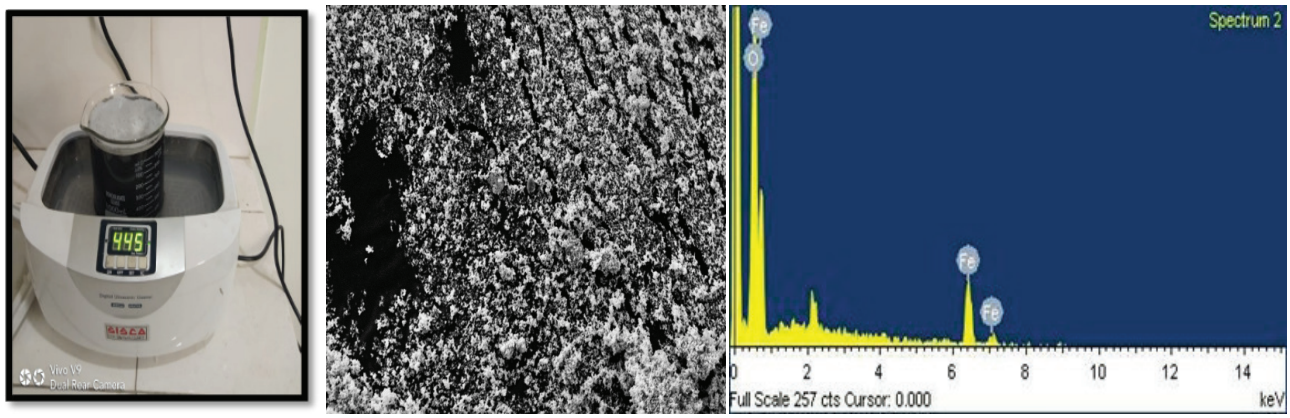

(a) **(b)** **(c)**

Figure 1. (a) Ultrasonic bath sonicator, **(b)** SEM image of Fe_3O_4, **(c)** EDAX image of Fe_3O_4.

Table 1. Details of the twisted tapes

S. no	Type	h/d
1	TT-1	3
2	TT-2	5
3	TT-3	7

tapes with different twist ratios represented with y= 3,5 and 7 is depicted in Figure 2.

Experimental Setup Description

Figure 3(a) depicts a photographic image of the experimental setup. It's a twin-type heat exchanger. The test segment consists of two copper pipes (inner) and one mild steel pipe

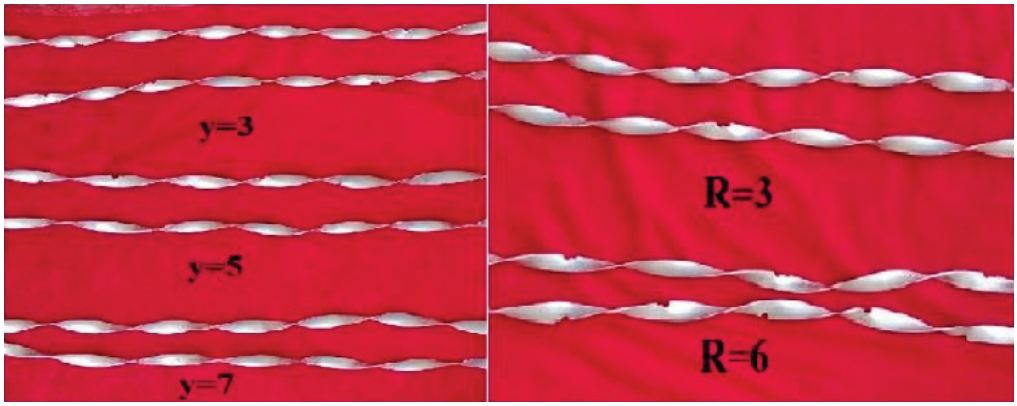

Figure 2. Variable cross-section twisted tapes with cut and different twist ratios (y=3, 5, 7) and variable-twisted tapes with cut radius, twist ratio 3 and distinct radii of cut (r=3, r=6).

Table 2. Specifications of the twin-pipe heat exchanger

Shell		Tubes	
Overall length	2.8m	Number of tubes	2
Outer diameter	0.063m	Length of tubes	5.6m
Inner diameter	0.060m	Effective heat transfer Area	0.53m^2
Effective heat transfer area	0.3m^2	Inner diameter	0.017m
		Outer diameter	0.019m

Figure 3. (a) Photographic view of experimental setup.

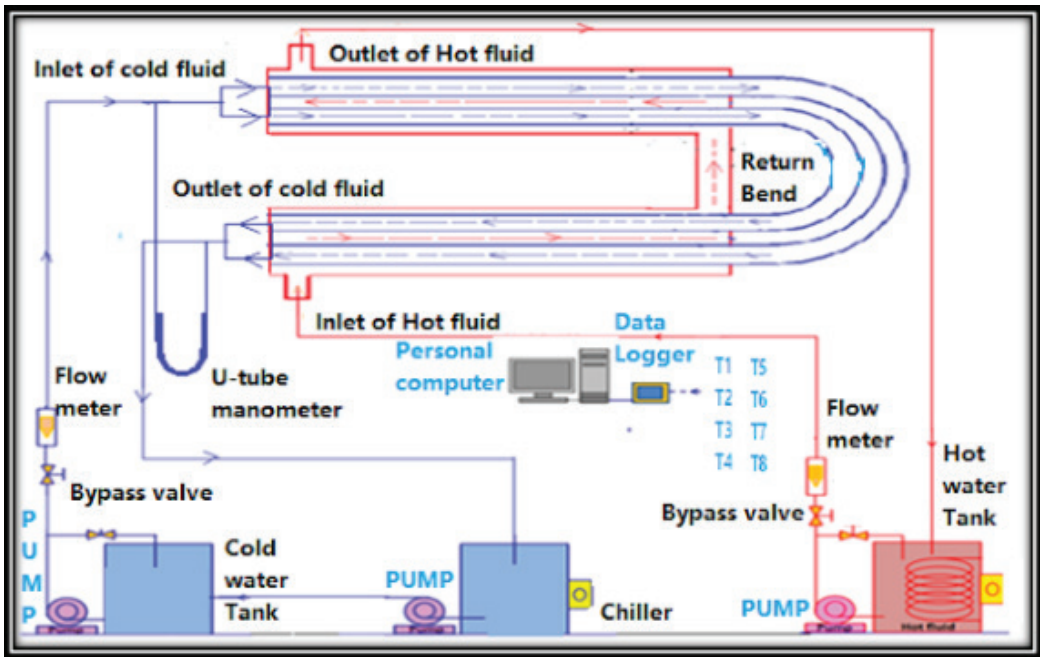

Figure 3. (b) Schematic layout of experimental setup.

(outer). The heat exchanger's specifications are listed in Table 2. A chiller, bypass valves, a manometer for measuring pressure loss in the test section, a tank for hot water, a tank for cold water, two pumps, thermocouples for measuring temperatures in the test section, flow meters on both the hot and cold sides for determining hot and cold water flow to the heat exchanger, and a tank each for hot and cold water. The schematic layout of the experimental setup is shown in Figure 3(b).

The instruments used for measuring various parameters during the trials include two rotameters for determining the flow rate of the hot and cold fluids, p-type thermocouples for measuring the inlet as well as the outlet temperatures and a U-tube mercury manometer for measuring the pressure of the cold fluid. The accuracy of rotameters (0-30 LPM) is in the range of ± 0.2-1% while thermocouples is ± 0.1°C.

The curve is designed to allow the fluid to re-circulate, allowing for efficient heat transfer. The annulus›s outer circumference is lacerated with asbestos rope. It is pierced to stop heat loss from the test portion to the surrounding environment. A pump circulates the hot fluid along the annulus, while the water or nanofluid circulates along the interior tube. Bypass valves manage cold and hot fluid flow rates. Flow meters of two in number were employed to determine the flow rates of the fluids of hot and cold types. The working fluid›s mass flow rate fluctuates in the range of 0.05 to 0.25 kg/s, while the heated fluid›s flow rate through the annulus is maintained constant at 0.1 kg/s.

The carrier fluid and nanofluid are circulated via the twin-pipe heat exchanger's interior pipe and measured with a cold fluid flow meter. In the annulus of the twin-pipe heat exchanger, hot fluid circulates. The temperatures of the hot and cold fluids at their input and outlet were evaluated by using four K-type thermocouples. The thermocouples are calibrated before they are used in the apparatus. The accuracy of the thermocouples was found to be 0.10 °C. The stainless steel hot and cold fluid tanks have a combined capacity of 30 liters. To avert heat loss from the hot water tank, it is wound with 0.06-meter-thick asbestos rope. A 1.5-KW heater is installed at the bottom of the tank to heat the hot water. The working fluids (water and nanofluid) are heated throughout the experiment and then passed through a chiller to cool to ambient temperature.After that, gravity returns the operating fluid to the cold water tank. In this case, the chiller is used to keep the operating fluid at room temperature. The pressure drop along the test section was measured with a U-tube manometer. Different flow rates of water, i.e., 0.083, 0.116, 0.15, and 0.25 kg/sec, were maintained in the experiments. The test segment receives a mass flow rate of 0.1 kg/sec of hot water. At the steady state, readings were taken. The cold fluid's flow rate is managed by the regulating valve. After the hot fluid achieved a consistent temperature of 600 °C, the temperature of the cold fluid entrance was measured.

Data Reduction

At steady-state conditions, heat rejected from the hot fluid is 6.13% greater than heat rejected from the cold fluid after accounting for equipment losses to the atmosphere. Average values of the cold and hot fluids are considered for further analysis. The average heat transfer is calculated using Syam Sundar et al. [22]

$$Q_{avg} = \frac{Q_h + Q_c}{2} \tag{3}$$

Where, Q_h= Heat transfer rate of hot fluid

Q_c = Heat transfer rate of cold fluid

The equation to determine Ui is given by Syam Sundar et al. [22]

$$Q_{avg} = U_i \times A_i \times \Delta T_{LMTD} \tag{4}$$

Where, U_i = inside overall heat transfer co-efficient

Ai= Heat transfer area inside

ΔT_{LMTD} = Log mean temperature difference

The inner heat transfer coefficient can be determined using Syam Sundar et al. [22]

$$\frac{1}{U_i} = \frac{1}{h_i} + \frac{d_0}{K}\ln\left(\frac{d_0}{d_i}\right) + \frac{d_i}{d_0}\frac{1}{h_0} \tag{5}$$

Where, h_i = heat transfer co-efficient inside

h_o = heat transfer co-efficient outside

d_i = inside diameter of tube

d_o= outside diameter of tube

Nusselt number for the base fluid can be determined by Syam Sundar et al. [22]

$$Nu = \frac{h_i \times d_i}{K_{bf}} \tag{6}$$

Where, k_{bf} = Thermal conductivity of base fluid

Frictionalfactor can be assessed by Syam Sundar et al. [22]

$$f = \frac{\Delta p \times 2 \times d}{L \times \rho \times v^2} \tag{7}$$

Where, Δp = Pressure drop

Nu can be evaluated with the help of using Syam Sundar et al. [22]

$$Nu_{nf} = \frac{h_{inf}}{k_{nf}} \tag{8}$$

Where, k_{nf} = Thermal conductivity of nanofluid

Where knf is assessed using Syam Sundar et al. [22]

$$k_{nf} = k_{bf}\frac{(k + 2k_f - 2\emptyset(k_f - K)}{K + 2k_f + \emptyset(k_f + K)} \tag{9}$$

Validation of Plain Pipe

The correlations for determining the Nusselt number of the plain tube are available in the literature which was developed by Gnielinski and Notter-Rouse. For turbulent flow, the Gnielinski correlation [31] is given by

$$Nu = \frac{(\frac{f}{2}) \times (Re - 1000) \times pr}{1.07 + 12.7 \times \left(\frac{f}{2}\right)^{0.5} \times (pr^{\frac{2}{3}} - 1)} \tag{10}$$

The correlation of Notter-Rouse [32] for finding Nu number in the flow regime of turbulent

$$Nu = 5 + 0.015 \times Re^{0.856} \times pr^{0.347} \tag{11}$$

Blasius correlation [33] for friction factor under turbulent flow regime

$$f = 0.3154 \times Re^{-0.25}, 3000 < Re < 105 \tag{12}$$

Petukhov correlation [34] for turbulent regime

$$f = (0.79 \times ln\,(Re) - 1.64)^{-2}, 2300 < Re < 106 \tag{13}$$

Uncertainty Analysis

To figure out the uncertainties in the trials suggested by Moffat [35], a systematic error analysis was performed. The parameters of the working fluids and the estimated uncertainties of the various instruments utilized are reported in Tables 3 and 4.

RESULTS AND DISCUSSION

Water was used as the carrier fluid in the preliminary trials. Eqs. (10) and (11) were used to compute the experimental nu and ff. Experimental Nusselt numbers were discriminated with Gnielinski and Notter-Rouse correlations to validate the setup. The variance of the experimental data with the aforementioned correlations is found to be within 5%. Figure 4 illustrates a disparity in the variation of experimental Nu for plain pipe with the data produced from the correlations.

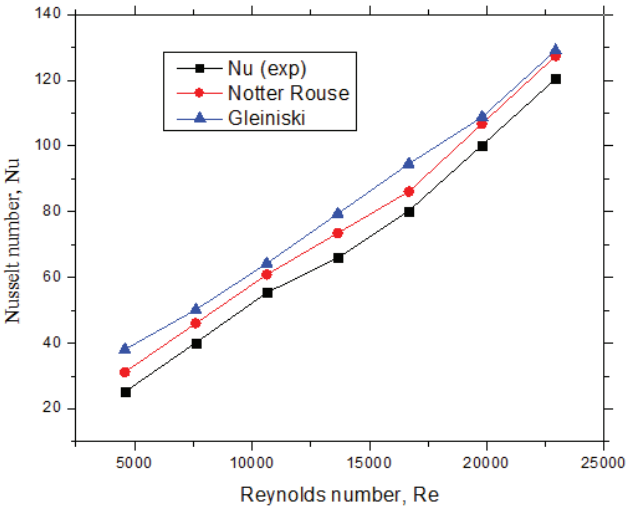

Figure 4. Experimental comparison of Gnielinski and Notter-Rouse with the water-based base fluid's Nusselt number.

Taguchi Optimization

In the current study, the Taguchi strategy of optimization was employed to evaluate results using Minitab software. As input attributes, flow rate, nanoparticle volume percentage, and cut radius were taken into account. While TPF, Nu, ff, and h were thought of as attributes of output, An L9 orthogonal array was employed to look into the implications of the input parameters. Additionally, S/N ratios have been generated using the ANOVA technique.

Table 3. Instruments uncertainties

S. No	Name of the Instrument	Range of the device	Parameter measured	Least count in measuring instrument	Min. and Max. values measured in the experiment	Uncertainty %
1	Thermocouple	0-1000°C	Tw	0.10 C	42.25-70.15	0.142
2	Thermocouple	0-1000°C	Tb	0.10 C	31.15-43.15	0.2317
3	Manometer	0-200 cm	h of the Mercury column	1 mm	2.0-80 cm	0.125
4	Flow meter	0-1000 L	m	1 L	1-15 L	0.66

Table 4. Uncertainty of different parameters

S. No	Name of the parameter	Uncertainty (%)
1	Heat transfer from hot fluid ,q_h	0.7066
2.	Heat transfer from cold fluid ,q_c	0.7066
3	Average Heat transfer from hot and cold fluids, Q_{avg}	1.4132
4	Logarithmic Mean temperature difference	0.401
5	Inner Overall Heat transfer coefficient, Ui	1.468
6	Outer Heat transfer coefficient, ho	0.72
7.	Inner Heat transfer coefficient, hi	1.638
8.	Nusselt number	1.641
9.	Reynolds number, Re	0.6675
10	Friction factor, f	0.947
11	Thermal performance factor, η	2.67

Table 5. L9 orthogonal array

Sl.	Flow rate (LPM)	Vol%	Cut radius	h (W/m2K)	Nu	TPF	ff
1	5	0.01	0	2043.82	52.66	1.042	0.0362
2	5	0.03	3	3354.56	85.55	1.151	0.0369
3	5	0.05	6	2445.19	61.11	1.189	0.0381
4	9	0.01	0	3061.70	76.52	1.066	0.0312
5	9	0.03	3	3195.73	82.33	1.135	0.0319
6	9	0.05	6	3509.84	89.51	1.241	0.0323
7	13	0.01	0	4180.75	106.62	1.063	0.0293
8	13	0.03	3	4628.69	126.32	1.231	0.0308
9	13	0.05	6	5054.28	119.26	1.171	0.0315

Table 6. S/N ratio performance parameters tables

Parameter	Level	Flow rate	Vol% of NP	Radius of cut
h	1	68.16	69.45	70.14
	2	70.24	71.30	71.44
	3	73.27	70.92	70.09
	Delta	5.11	1.85	1.34
	Rank	1	2	3
Nu	1	36.27	37.55	38.50
	2	38.34	39.66	39.28
	3	41.37	38.76	38.20
	Delta	5.11	2.11	1.09
	Rank	1	2	3
ff	1	28.62	29.87	29.62
	2	29.95	29.60	29.60
	3	30.31	29.41	29.66
	Delta	1.69	0.46	0.05
	Rank	1	2	3
TPF	1	1.0275	0.4811	1.3460
	2	1.1768	1.3755	1.0493
	3	1.2357	1.5834	1.0447
	Delta	0.2082	1.1023	0.3012
	Rank	3	1	2

The L9 orthogonal array and performance parameter ratio of S/N were represented in Tables 5 and 6.

Convective Heat Transfer Coefficient (h)

Figure 5(a) demonstrates the S/N ratio for convective heat transmission, with bigger values indicating better conditions. There is a significant increase in h by enhancing the flow rate, volume of nanofluid, and radius of cut. 6 tabulated the variable influence estimated via ANOVA. Among all these input parameters, radius of cut and volume of NP contributed 20.49 and 27.52 percent, respectively, whereas the flow rate of the coolant contributed the highest percentage of 50.29 percent. Figure 5(b) illustrates the residual model for h, which exhibits a confidence level of 96%. As the flow rate escalates, there is a note-worthy enhancement in heat transfer rate because the thickness of the boundary layer reduces, and the dispersal of nanoparticles also results in enhancement because of the Brownian motion of nanoparticles. The data obtained from the optimization reveals that the addition of nanoparticles to the base fluid shows a noteworthy impact on enhancement of convective heat transfer co-efficient is in good agreement with the data obtained from the experimental data because

the highest convective heat transfer co-efficient is obtained at highest Vol% of nanoparticles i.e. 0.05

Nusselt Number (Nu)

The Nusselt number S/N ratio is depicted in Figure 6(a), with a bigger value indicating a more favourable condition. By increasing the flow rate, volume of nanofluid, and radius of cut, Nu is significantly increased. ANOVA anticipated parameter contribution was tabulated in 6. Among all these input parameters, Radius of cut and Vol% NP contributed 12.87 and 34.25%, respectively, whereas the flow rate of the coolant contributed the highest% of 50.34. Figure 6(b) shows the residual model for NU with a confidence level of 96%. As k of the fluid increases due to the addition of ferric oxide nanoparticles, the convective heat transfer coefficient of the nanoparticle-dispersed fluid increases. Substantial enhancement of the convective heat transfer coefficient of fluid results in a surge in h. The maximum increase in the Nusselt number for 0.05 percent nanofluid concentration and VCRTT of radius of cut 6 is 42.01 percent over the smooth pipe were obtained during the trials and the optimization results also reveals that addition of nanoparticles and radius of cut had a significant impact in enhancement of Nusselt number.

Friction Factor (ff)

The friction factor S/N ratio is depicted in Figure 7(a), where the lower the value, the more favourable the circumstance. By increasing the flow rate, volume of nanofluid, and radius of cut, ff is significantly increased. ANOVA assessed variable influence was tabulated in 6. Among all these input parameters, radius of cut and volume of NP contributed 3.66 and 14.65%, respectively, whereas the flow rate of the coolant contributed the highest percentage of 60.69. Figure 7(b) shows the residual model for ff with a certainty level of 96%. From the trials, it was observed that dispersion of nanoparticles results in a slight enhancement in the viscosity of nanofluid. As the viscosity of the nano dispersed fluid rises, the decrease in friction factor is low.

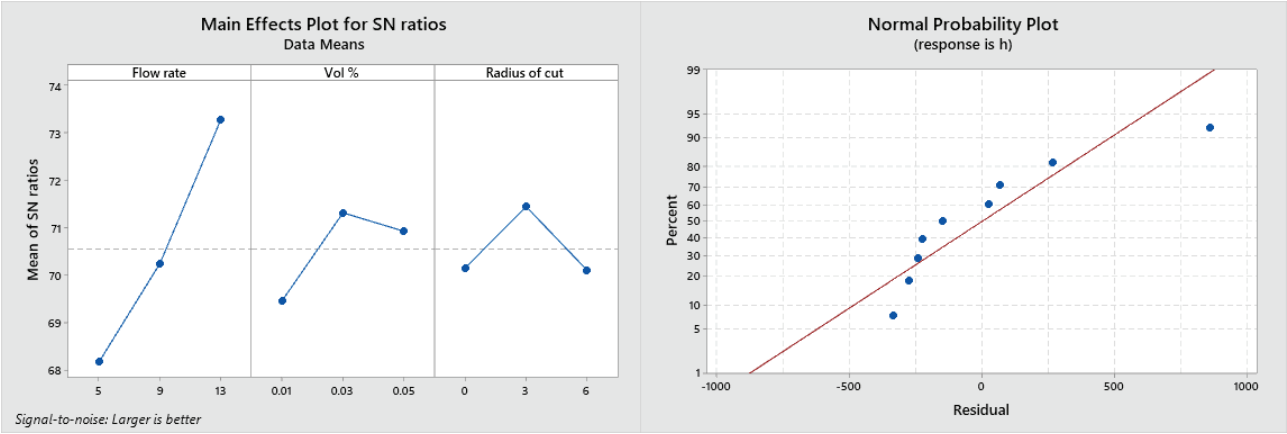

Figure 5. **(a)** h S/N ratio and **(b)** h residual model.

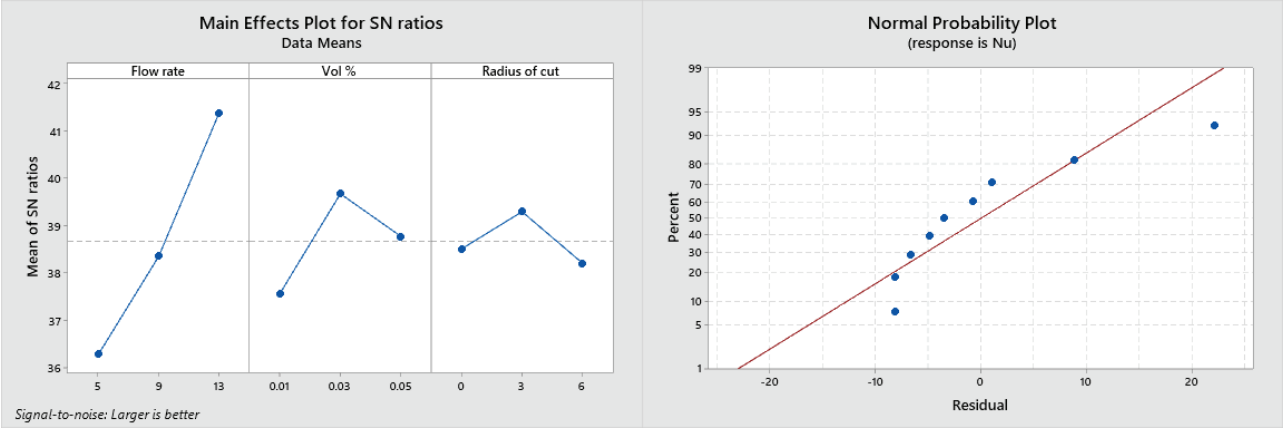

Figure 6. **(a)** Nu S/N ratios and **(b)** Nu residual model.

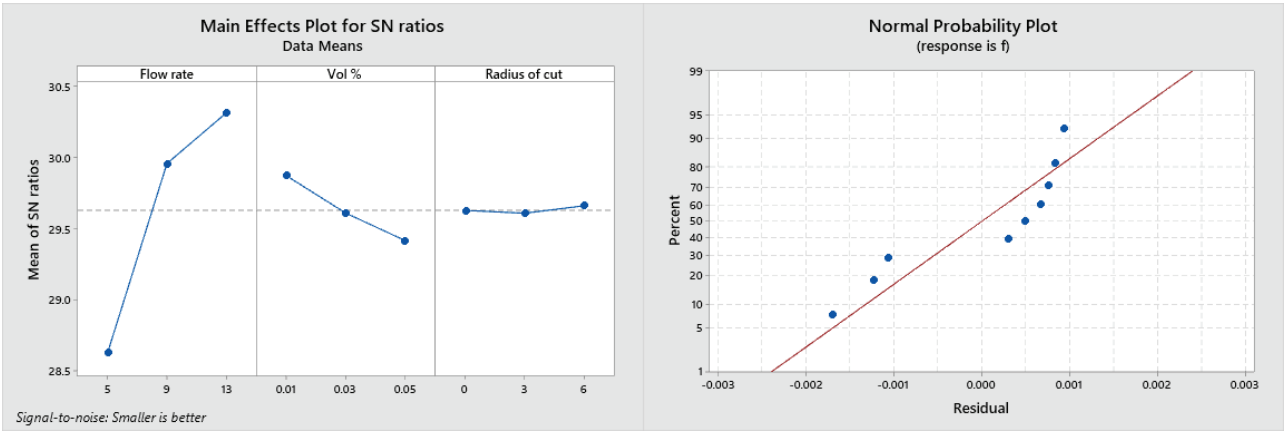

Figure (7). (a) ff S/N ratio and **(b)** ff residual model.

Thermal Performance Factor (TPF)

Figure 8(a) depicts the S/N ratio for the thermal performance parameter, with the larger value indicating a better condition. There is a significant increase in TPF by enhancing the flow rate, volume percent of nanofluid, and radius of cut. The thermal performance factor was greatly influenced by the addition of nanoparticles to the fluid. ANOVA assessed the variable effect and was tabulated in 6. Among all these input parameters contributed by the Vol% of NP, the radius of the cut and flow rate of the coolant are 79.75, 4.37, and 3.83%, respectively. The residual model was displayed in Figure 8(b) with a confidence level of 96%. As the addition of nanoparticles results in a greatly influenced surge in the thermal performance factor, it is because of various mechanisms of Brownian motion, rotation of particles, thermophoretic motion, etc. The impingement of nanoparticles makes an upsurge in thermal performance factor shown in Taguchi was in agreement with experimental data because during the trials the highest thermal performance factor i.e. was obtained at 0.03 % Ferric oxide nanofluid with twisted tapes 1.29 (Table 7).

Optimization Through ANN

Artificial neural networks are an improved approach compared with the Taguchi approach, which depends on how the neurons in humans operate. ANN is a mathematical framework when examined in the context of the design of neurons. It links data and results by altering the relationships among the inner nodes. ANN is useful in regulating an intricate relationship that is nonlinear and forecasting yield in conjunction with the recurring nature of previous data in the search region. ANN consists of three various layers, normally the input layer, the intermediate layer, and the output layer. In the input layer, initial data for the neural network will be provided; all the computation will be done at the intermediate layer, and the result will be obtained at the outer layer.

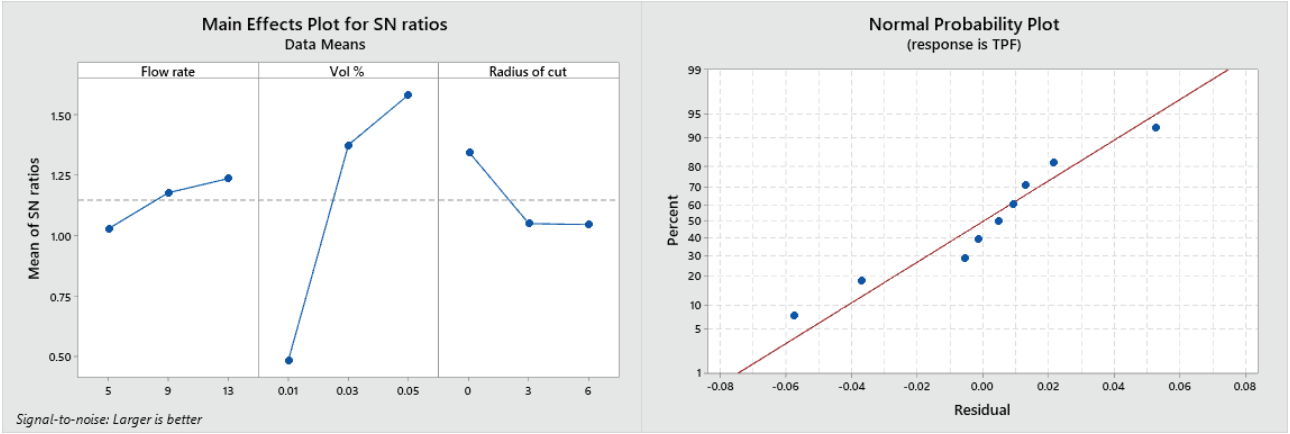

Figure 8. (a) TPF S/N ratios and **(b)** TPF residual model.

Table 7. ANOVA for S/N ratio execution parameters

Parameter	Source	DF	Adj SS	Adj MS	F-Value	P-Value	Contribution (%)
H	Regression	3	6556860	2185620	9.63	0.016	
	Flow rate	1	6040368	6040368	26.60	0.004	50.29
	Vol %	1	494811	494811	2.18	0.200	27.52
	Radius of cut	1	21682	21682	0.10	0.770	20.49
	Error	5	1135237	227047			1.71
	Total	8	7692097				100.00
Nu	Regression	3	4145.57	1381.86	8.81	0.019	
	Flow rate	1	3895.38	3895.38	24.84	0.004	50.34
	Vol %	1	193.57	193.57	1.23	0.317	34.25
	Radius of cut	1	56.61	56.61	0.36	0.574	12.87
	Error	5	784.06	156.81			2.25
	Total	8	4929.62				100.00
F	Regression	3	0.000069	0.000023	13.46	0.008	
	Flow rate	1	0.000064	0.000064	37.72	0.002	60.69
	Vol %	1	0.000005	0.000005	2.66	0.164	14.65
	Radius of cut	1	0.000000	0.000000	0.00	1.000	3.66
	Error	5	0.000008	0.000002			2.00
	Total	8	0.000077				100.00
TPF	Regression	3	0.034653	0.011551	7.00	0.031	
	Flow rate	1	0.001148	0.001148	0.70	0.442	79.75
	Vol %	1	0.030817	0.030817	18.67	0.008	3.83
	Radius of cut	1	0.002688	0.002688	1.63	0.258	4.37
	Error	5	0.008253	0.001651			2.04
	Total	8	0.042906				100.00

Table 8. ANN results

Hidden Layers	Neurons	Training	Validation	Testing	All
1	10	0.98412	0.99984	0.99993	0.9544
1	20	1	0.9999	1	0.9992
1	30	0.94295	0.99989	0.99998	0.95197

This work considered feed-forward back propagation neural networks, which had input, hidden, and output layers, respectively. Of the training algorithms available in the ANN tool in Matlab, the Levenberg-Marquardt approach was the one that was widely used. In order to minimize the mean square error, it uses a back propagation approach to contrast its output to the needed target output. It works more effectively for non-linear regression problems and is the fastest method. The LMA was used to assist in training the model. In the current work, the tansig transfer function was used. The transfer function in the first layer is tan-sigmoid, and the output layer transfer function is linear. Trial and error was used to identify the number of neurons until the mean-square error (MSE) was as low as possible. From 10 to 30 neurons were present. 20 neurons were used to reach the optimal values. The information about the data obtained from ANN is demonstrated in Figure 9. It was observed from the graph that most of the data relates to X = Y. Then the data obtained from ANN is in good agreement with the experimental data. Figure 10 shows the architecture of ANN at 20 neurons. ANN results for each neuron in the range of 10, 20 and 3 (Table 8).

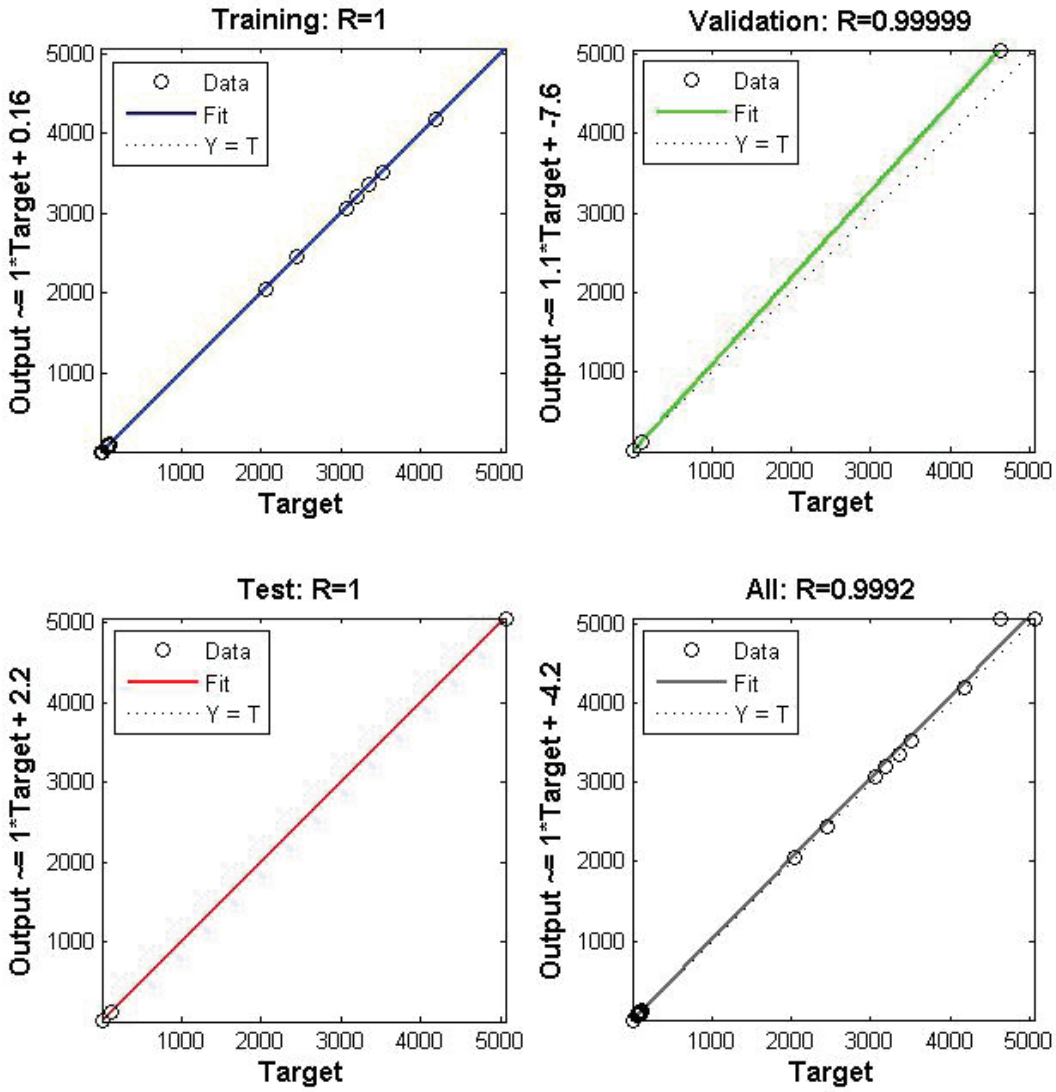

Figure 9. Data obtained from ANN at 20 neurons.

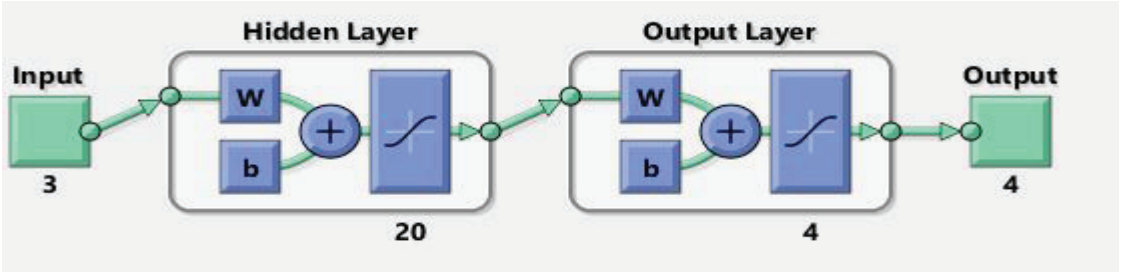

Figure 10. Architecture of ANN at 20 neurons.

CONCLUSION

An experimental study was done by placing the twisted tapes and passing a ferric oxide nanofluid into a twin-pipe heat exchanger. During the experimental study, the flow rate of the coolant, the volume percentage of nanoparticles, and the radius of the cut were altered. In addition to that, optimization techniques like Taguchi, ANOVA, and ANN were applied to the trial data, and significant observations were drawn below. An experimental study reveals that the addition of nanoparticles and the radius of cut play a significant

role in the enhancement of heat transfer parameters like h, Nu, ff, and the thermal performance factor when compared with a base fluid. The thermal performance factor was highly enhanced, mainly due to the variation in the radius of the cut and the addition of nanoparticles. The Taguchi technique was applied to the experimental data. For the parameters h, Nu, and thermal performance factor, the larger is better condition was used, while the smaller is better condition was used for the ff. The flow rate of the coolant and the volume of nanoparticles, with values of 50.29 and 27.32%, respectively, improved the convective heat transfer coefficient parameter. The flow rate of the coolant and the volume percent of NP, which were 50.34 and 34.25 percent, were influencing parameters in the enhancement of Nu. The parameters Vol% of NP and Radius of Cut, with %s of 79.75 and 3.83, had a significant influence on the thermal performance factor. The results obtained from the Taguchi and ANN were in good agreement with the experimental data. Results revealed that there is an enhancement in the thermal performance of a heat exchanger with variable twisted tapes and nanofluid. There is always a need for heat exchangers with increased heat transfer rates to reduce cross sections for industrial applications. Consequently, the heat exchanger employed in this study has prospective uses in the fields of industrial processing, renewable energy, and other engineering domains.

NOMENCLATURE

DPHE	Double pipe heat exchanger
D	Nanoparticles crystalline size
di	inner diameter of tube,m
do	outer diameter of tube, m.
ff	friction factor
h	Convective-heat transfer coefficient (W/m2K)
K	Scherrer constant
LAM	Levenberg-Marquardt Algorithm
m	mass flow rate (kg/s)
Nu	Nusselt number
Re	Reynolds number
T	temperature (K)
TPF	Thermal performance Reynolds number factor
Thi	hot fluid inlet temperature
Tci	cold fluid inlet temperature

Greek Abbreviation

θ	Bragg Angle
β	Full width at half maximum
μ	Viscosity, kg/m.s
ϕ	Vol% of nanoparticles
ΔT	temperature difference between inlet and outlet, K
ρ	density (kg/m3)
λ	Wavelength

Subscripts

bf	base fluid
c	cold side
h	hot side
nf	Nanofluid

AUTHORSHIP CONTRIBUTIONS

Authors equally contributed to this work.

DATA AVAILABILITY STATEMENT

The authors confirm that the data that supports the findings of this study are available within the article. Raw data that support the finding of this study are available from the corresponding author, upon reasonable request.

CONFLICT OF INTEREST

The author declared no potential conflicts of interest with respect to the research, authorship, and/or publication of this article.

ETHICS

There are no ethical issues with the publication of this manuscript.

REFERENCES

[1] Bergles AE. The implications and challenges of enhanced heat transfer for the chemical process industries. Chem Engineer Res Des 2011;79:437-444. [CrossRef]

[2] Buongiorno J. Convective transport in nanofluids. Trans ASME 2006;128:240-250. [CrossRef]

[3] Godson LB, Lal DM, Wongwises S. Enhancement of heat transfer using nanofluids-An overview. Renew Sustain Energy Rev 2010;214:629-641. [CrossRef]

[4] Bozorg Bigedli M, Fasano M, Cardellini A, Chivazzo E, Asinari P. A review on the heat and mass transfer phenomena in nanofluid coolants with a special focus on automotive applications. Renew Sustain Energy Rev 2016;60:1615-1633. [CrossRef]

[5] Kakac S, Pramuanjaroenkij A. Review of convective heat transfer enhancement with nanofluids. Int J Heat Mass Transf 2009;52:3187-3196. [CrossRef]

[6] Sarafraz MM, Hormozi F, Peyghambarzadeh SM. Thermal performance and efficiency of a thermosyphon heat pipe working with a biologically ecofriendly nanofluid. Int Comm Heat Mass Transf 2014;57:297-303. [CrossRef]

[7] Sarafraz MM, Tian Z, Tlili I, Kazi S, Goodarzi M. Thermal evaluation of a heat pipe working with n-pentane-acetone and n-pentane-methanol binary mixtures. J Therm Anal Calorim 2020;139:2435-2445. [CrossRef]

[8] Shima PD, Philip J, Raj B. Synthesis of aqueous and nonaqueous iron oxide nanofluids and study of temperature dependence on thermal conductivity and viscosity. J Phys Chem C 2010;114:18825-18833. [CrossRef]

[9] Chopkar M, Das PK, Manna I. Synthesis and characterization of nanofluid for advanced heat transfer applications. Scr Mater 2006;55:549-552. [CrossRef]
[10] Parekh K, Lee HS. Magnetic field induced enhancement in thermal conductivity of magnetite nanofluid. J Appl Phys 2010;107:09A310. [CrossRef]
[11] Syam Sundar L, Abebaw HM, Singh KM, Pereira AMB, Sousa AMC. Experimental heat transfer and friction factor of Fe3O4 magnetic nanofluids flow in a tube under laminar flow at high Prandtl numbers. Int J Heat Technol 2020;36:301-313. [CrossRef]
[12] Han D, He WF, Asif FZ. Experimental study of heat transfer enhancement using nanofluid in double tube heat exchanger. Energy Procedia 2017;142:2547-2553. [CrossRef]
[13] Guan BH, Hanafi M, Khalid M, Matraji HH, Chuan LK, Soleimani H. An evaluation of iron oxide nanofluids in enhanced oil recovery application. AIP Conf Proc 2014;1621:600-604. [CrossRef]
[14] Elsaidy A, Vallejo JP, Salgueirino V, Lugo L. Tuning the thermal properties of aqueous nanofluids by taking advantage of size-customized clusters of iron oxide nanoparticles. J Mol Liq 2021;344:117727. [CrossRef]
[15] Sarma PK, Kishore PS, Dharma Rao V, Subrahmanyam T. A combined approach to predict coefficients and convective heat transfer characteristics in a tube with twisted tape inserts for a wide range of Re and Pr. Int J Therm Sci 2005;44:393-398. [CrossRef]
[16] Syam Sundar L, Sharma KV. Turbulent heat transfer and friction factor of Al2O3 nanofluid in a circular tube with twisted tape inserts. Int J Heat Mass Transf 2010;53:1409-1416. [CrossRef]
[17] Sarma PK, Kedarnath C, Sharma KV, Syam Sundar L, Kishore PS, Srinivas V. Experimental study to predict momentum and thermal diffusivities from convective heat transfer data of nano fluid with Al2O3 dispersion. Int J Heat Technol 2010;28:123-131.
[18] Sadeghi O, Mohammed HA, Bakhtiari-Nejad M, Wahid MA. Heat transfer and nanofluid flow characteristics through a circular tube fitted with helical tape inserts. Int Commun Heat Mass Transf 2016;71:234-244. [CrossRef]
[19] Sarma PK, Kedarnath C, Dharma Rao V, Kishore PS, Subrahmanyam T, Bergles AE. Evaluation of momentum and thermal eddy diffusivities for turbulent flow in tubes. Int J Heat Mass Transf 2010;53:1237-1242. [CrossRef]
[20] Varma KV, Pisipaty SK, Mendu S, Ghosh R. Optimization of performance parameters of a double pipe heat exchanger with cut twisted tapes using CFD and RSM. Chem Eng Process Process Intensif 2021;163:108362. [CrossRef]
[21] Kelidari M, Maoghadam AJ. Effects of Fe3O4/water nanofluid on the efficiency of a curved pipe. J Therm Sci Engineer Appl 2019;4:041016. [CrossRef]
[22] Syam Sundar L, Kumar NT, Naik MT, Sharma KV. Effect of full-length twisted tape inserts on heat transfer and friction factor enhancement with Fe3O4 magnetic nanofluid inside a plain tube: An experimental study. Int J Heat Mass Transf 2012;55:2761-2768. [CrossRef]
[23] Aghayari R, Maddah H, Ashori F, Hakiminejad A, Aghili M. Effect of nanoparticles on heat transfer in mini double-pipe heat exchangers in turbulent flow. Heat Mass Transf 2015;51:301-306. [CrossRef]
[24] Aghayari R, Maddah H, Baghbani Arani J, Mohammadiun H, Nikpanje E. An experimental investigation of heat transfer of Fe2O3/water nanofluid in a double pipe heat exchanger. Int J Nano Dimens 2015;6:517-524.
[25] Wijayanta AT, Pranowo, Mirmanto, Kristiwan B, Aziz M. Internal flow in an enhanced tube having square-cut twisted tape insert. Energies 2019;12:306. [CrossRef]
[26] Al-Obaidi AR. Investigation of thermal flow structure and performance heat transfer in a three-dimensional circular pipe using twisted tape based on Taguchi method analysis. Heat Transf 2021;51:1649-1659. [CrossRef]
[27] Kumar V, Sahoo RR. Parametric and design optimization investigation of a wavy fin and tube air heat exchanger using the T-G technique. Heat Transf 2022;51:4641-4666. [CrossRef]
[28] Kavitha R, Abd Algani YM, Kulkarni K, Gupta MK. Heat transfer enhancement in a double pipe heat exchanger with copper oxide nanofluid: An experimental study. Mater Today Proc 2022;56:3446-3449. [CrossRef]
[29] Praveenkumara BM, Gowda BS, Bharatwaj KN. An experimental investigation of study the combined effect of threaded pipe and twisted tap inserts on heat transfer rate of double pipe heat exchangers. Mater Today Proc 2023;82:108-117. [CrossRef]
[30] Colaco AB, Mariani VC, Salem MR, Coelho LD. Maximizing the thermal performance index applying evolutionary multi-objective optimization approaches for a double pipe heat exchanger. Appl Therm Engineer 2022;211:118504. [CrossRef]
[31] Gnielinski V. New equations for heat and mass transfer in turbulent pipe and channel flow. Int Chem Engineer 1976;16:359-368.
[32] Notter RH, Rouse MW. A solution to the Graetz problem - III, Fully developed region heat transfer rates. Chem Engineer Sci 1972;27:2073-2093. [CrossRef]
[33] Blasius B. Boundary layers in fluids with small friction. Z Math Phys 1908;56:1-37.
[34] Petukhov BS. Heat transfer and friction in turbulent pipe flow with variable physical properties. Adv Heat Transf 1970;504-564. [CrossRef]
[35] Moffat RJ. Describing the uncertainties in experimental results. Exp Therm Fluid Sci 1988;1:3-17. [CrossRef]